

European Journal of Immunology

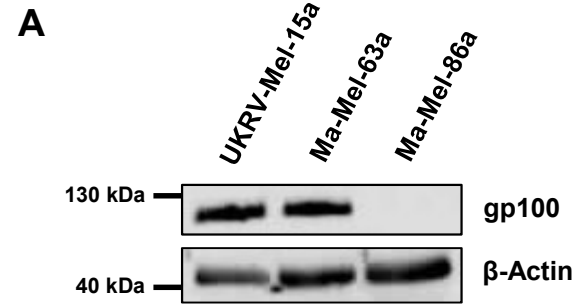
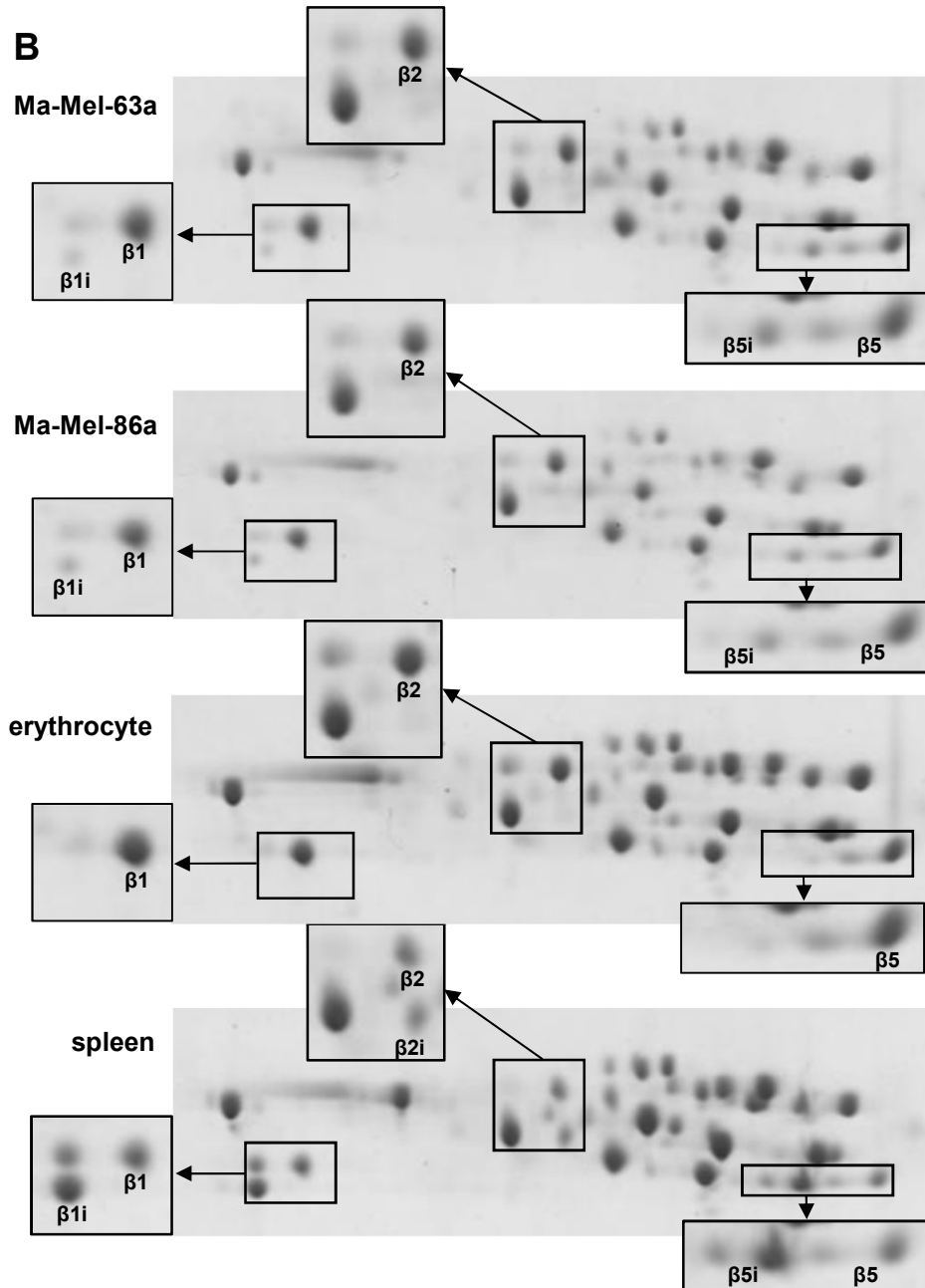
Supporting Information

for

DOI 10.1002/eji.201948116

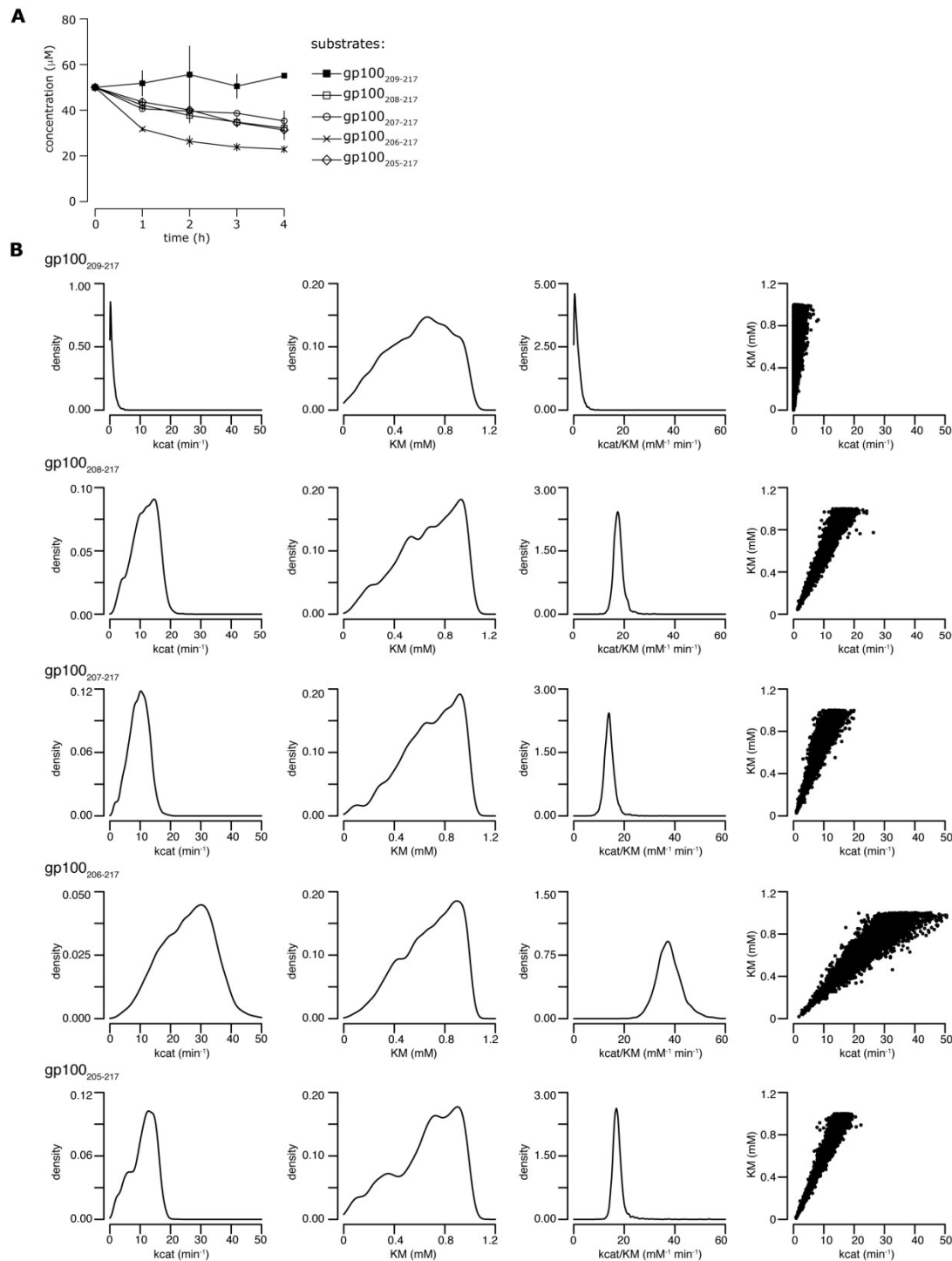
Kathrin Textoris-Taube, Clemens Cammann, Petra Henklein, Eyllin Topfstedt, Frédéric Ebstein, Sarah Henze, Juliane Liepe, Fang Zhao, Dirk Schadendorf, Burkhardt Dahlmann, Wolfgang Uckert, Annette Paschen, Michele Mishto and Ulrike Seifert

ER-aminopeptidase 1 determines the processing and presentation of an immunotherapy-relevant melanoma epitope



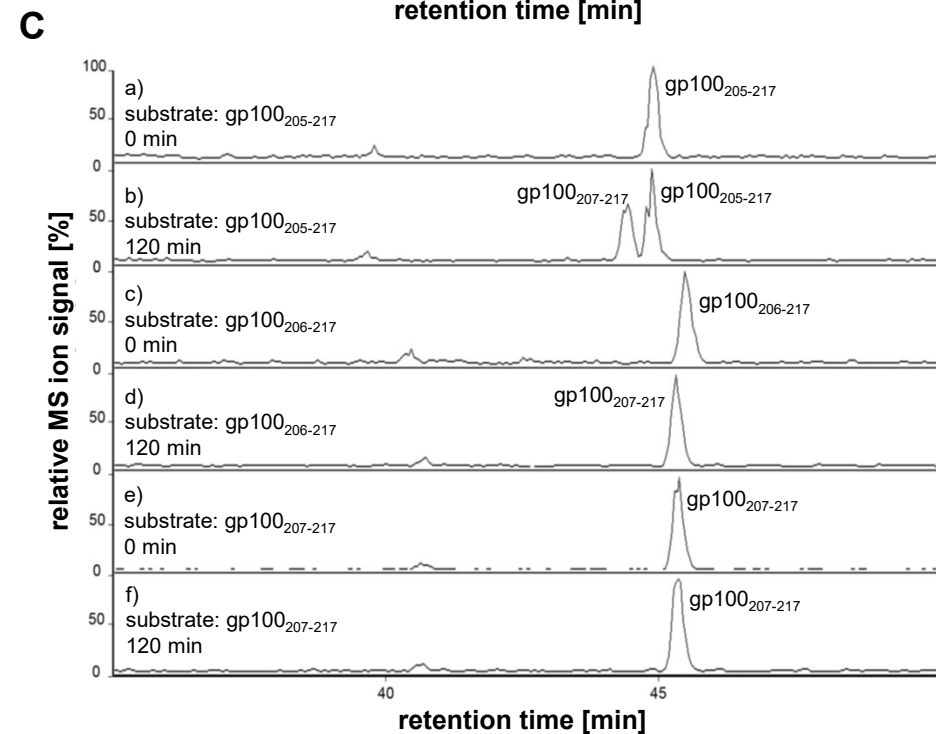
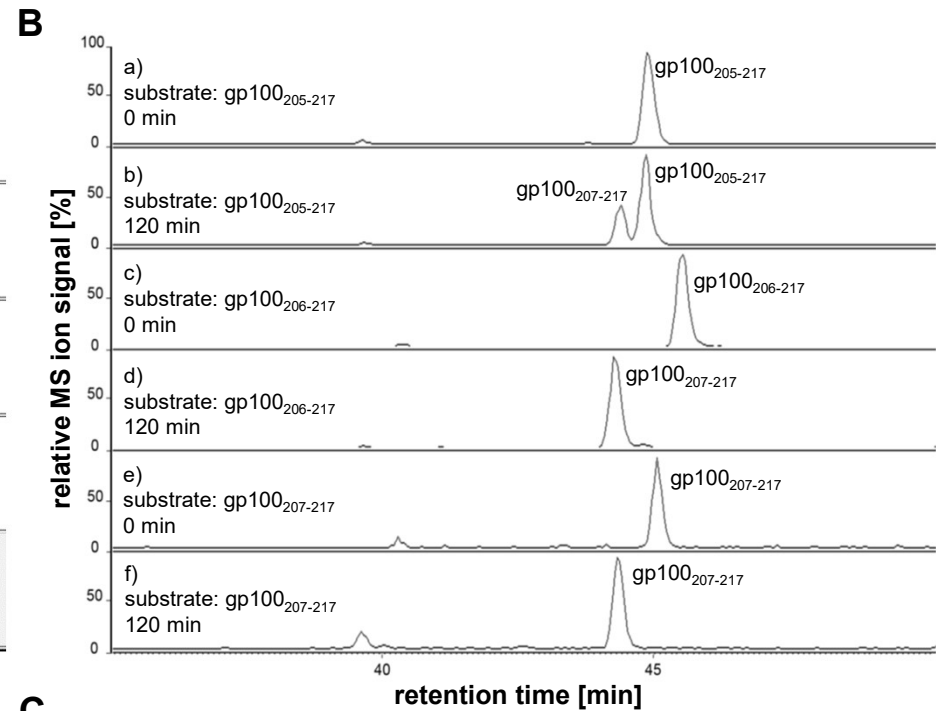
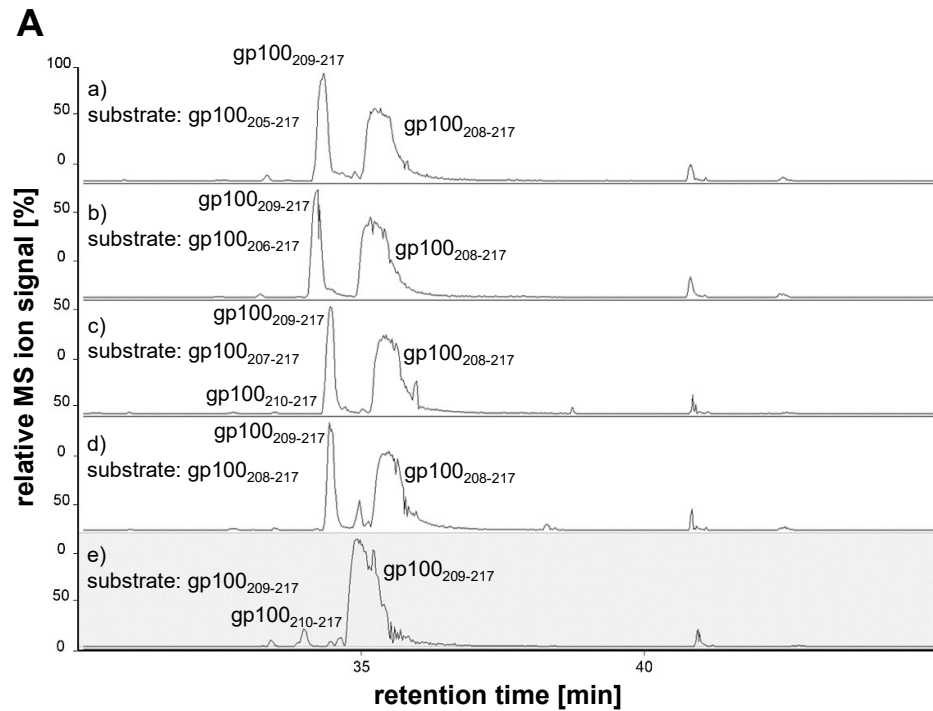
Supporting Information Figure 1. Subunit composition of 20S proteasomes isolated from human melanoma cells.

(A) Gp100 expression in melanoma cells (one out of two independent experiments). (B) Subunits of the isolated 20S proteasome complexes from melanoma cell lysates were identified by two-dimensional gel electrophoresis and Coomassie blue staining. Proteasomes isolated from human erythrocytes and spleen served as control for standard proteasome and immunoproteasome. The location of $\beta 1/\delta$ and $\beta 1i/LMP2$, $\beta 2/Z$ and $\beta 2i/MECL-1$, $\beta 5/MB1$ and $\beta 5i/LMP7$ are enlarged (1,5 times) and marked with arrows. One representative experiment.



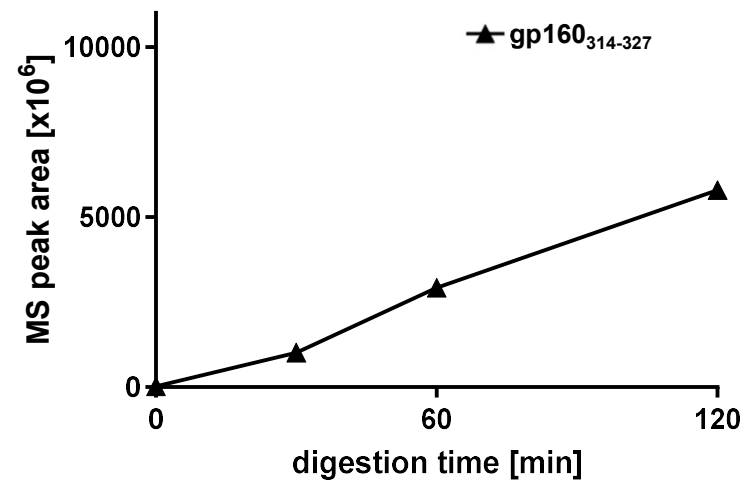
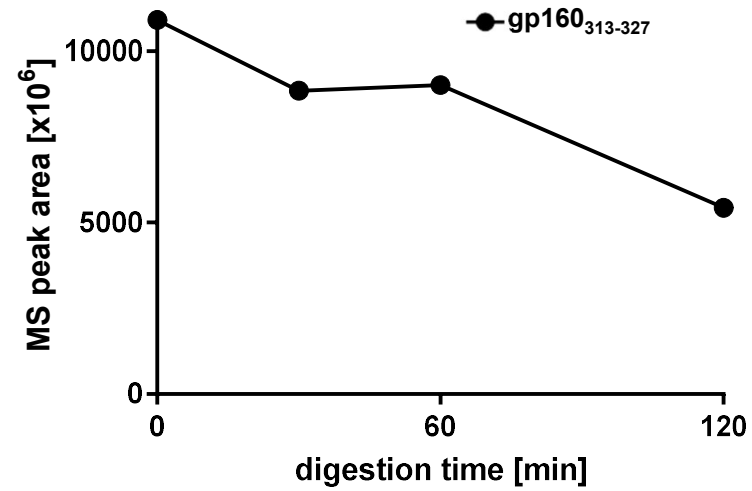
Supporting Information Figure 2. ERAP-1-mediated trimming of synthetic gp100 peptides.

(A) Quantitative kinetics of the degradation of the gp100-derived synthetic peptides by ERAP1. Values are the mean and SD of 2 independent experiments previously published (Textoris-Taube et al., 2015). Substrate quantification was carried out through peptide titration. (B) Estimation of kinetic parameters based on Michaelis-Menten model using Bayesian inference in a Markov Chain Monte Carlo scheme. Shown are the marginal posterior parameter distributions for k_{cat} , K_{M} and $k_{\text{cat}}/K_{\text{M}}$. Furthermore, scatterplots of K_{M} vs k_{cat} are shown and indicate strong correlation between the two parameters, allowing to calculate their ratio $k_{\text{cat}}/K_{\text{M}}$ with densities plotted.

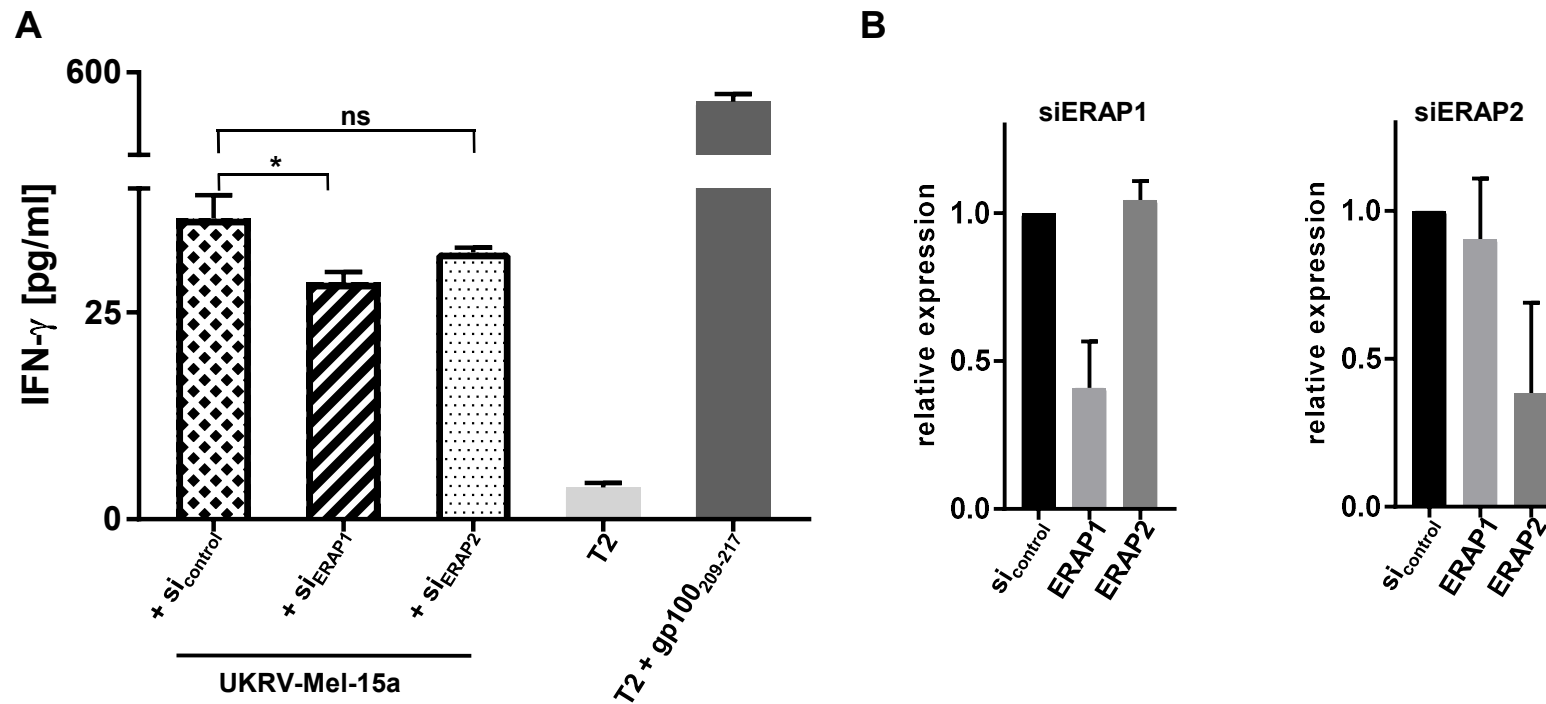


Supporting Information Figure 3. Peptides produced by different amounts of ERAP1 and ERAP2.

(A-C) LC-MS HPLC profiles, representative of 2 independent experiments, of the substrates and peptide products identified in the *in vitro* digestions carried out with (A) 2 µg ERAP1 for 4 h (the epitope is marked in grey, the HPLC-profile is zoomed from 30 to 45 min), (B) 3 ng ERAP2 for 2 h and (C) 2 µg ERAP2 for 2 h. The HPLC-profiles are zoomed from 35 to 50 min.

A**B**

Supporting Information Figure 4. Activity control of recombinant ERAP2. (A and B) The epitope precursor peptide HIV glycoprotein (gp)160₃₁₃₋₃₂₇ containing the epitope GPGRAFVTI was digested *in vitro* for the indicated time points by ERAP2 3 ng/20 μ l. Peptide fragment gp160₃₁₄₋₃₂₇ generation by cleavage after K₃₁₃ is indicated, which was previously shown to be mediated by ERAP2 [17]. The graphical plots show MS signal measured in ion current versus incubation time (one out of two technical replicates is displayed).



Supporting Information Figure 5. Altered activation of gp100₂₀₉₋₂₁₇-specific CTL clones upon ERAP1 siRNA in UKRV-Mel-15a cells.

(A) IFN- γ -production of gp100₂₀₉₋₂₁₇-specific CTL clones incubated for 16 h with UKRV-Mel-15a melanoma cells expressing HLA-A*02:01 and the gp100 antigen. UKRV-Mel-15a cells were pre-treated with 100 nM ERAP1, ERAP2 or control siRNA for 72h. T2 cells served as negative and gp100₂₀₉₋₂₁₇-peptide loaded T2 cells as positive control, the mean and the SD of three technical replicates are shown. Student's t-test; $p < 0.05$. (B) qPCR analysis of ERAP1 and ERAP2 down-regulation in UKRV-Mel-15a cells. Relative expression was calculated in comparison to control siRNA treated cells and 18S rRNA served as housekeeping gene. The means and SD of three technical replicates are shown. One out of two independent experiments is shown (A-B).